Himalayan Geology, Vol. 27 (2), 2006, pp. 95-110, Printed in India

Numerical Modelling of Graben Faults with Special Reference to Thakkhola Half Graben, Central Nepal Himalaya

DEEPAK CHAMLAGAIN*, DAIGORO HAYASHI
Department of Physics and Earth Sciences, University of the Ryukyus, Okinawa, 903-0213, Japan
** E-mail: dchamlagain@hotmail.com*

Abstract: Thakkhola half graben is a product of Late Cenozoic extensional tectonics in the Himalaya-Tibetan region. A series of 2D finite element models are generated to simulate its first order characteristics using stress field and induced fault pattern as structural proxies. Extensional graben faults form in the upper weak layer and propagate downward with increasing extension. Clusters of failure elements at the two ends of the graben directly correspond to the graben bounding faults and the asymmetric feature is characterized by uneven development of faults therein. The syntectonic deposits are characterized by normal fauls in the tensional stress field, which is a common feature of the small-scale graben at post rift deformation stage. The proposed models suggest that depth of a graben growth fault is primarily controlled by the initial fault and density of the syntectonic deposits. Assumption of a weak zone (Thakkhola fault system) does not make significant difference in stress distribution and faulting. It is thus suggested that a weak zone only can not contribute to the development of a half graben. The spreading boundary condition could not simulate the existing fault configuration in the Thakkhola half graben. Our modelling results for the graben suggest gravitational collapse of the elevated plateau rather than mantle upwelling during spreading.

INTRODUCTION

Normal faults indicating east-west extension are distributed throughout the southern half of the Tibetan Plateau and crest of the Himalaya (Fig. 1). Since their discovery (Molnar & Tapponier 1978), earth scientists have been studying on the origin of these grabens, which are seemingly enigmatic features in a regionally compressional tectonic setting between the colliding plates. Some of the possible explanations include: (1) gravitational spreading of the elevated plateau driven by excess gravitational potential energy (Molnar & Tapponier 1978) (2) extension in response to regional conjugate strike slip faulting associated with eastward extrusion of Tibet (Armijo *et al.* 1986), (3) isostatic response to erosion of the mantle lithosphere (England & Houseman 1989), (4) Lower crustal flow (Royden *et al.* 1997), (5) oblique convergence between India and Eurasia (McCaferry & Nabelek 1998), (6) arc-parallel extension (Seeber & Pecher 1998), and (7) middle Tertiary mantle upwelling in eastern Asia that induced thermal weakening of the lithosphere (Yin 2000).

Thakkhola half graben (Figs. 1 and 2) is one of many north trending grabens that define the Neogene structural pattern of the southern margin of the Tibetan Plateau. Lying to the southern boundary of the Tibetan Plateau and near the crest of the Himalaya, it provides an ample opportunity to understand the east-west extension in Tibet and E-W extensional strain in the Himalaya. In this study we aim to simulate the first order characteristics of the Thakkhola half graben using different geometries, boundary conditions and rock layer properties. Further this study constrains the probable mechanical properties for the Thakkhola half graben. Finally, efforts are being made to explain the genesis of the Thakkhola half graben using the available geological data and simulated numerical models.

Regional Characteristics of Grabens of the Himalaya-Tibet Orogen

Grabens of Tibet and the Himalaya represent the Cenozoic extensional tectonic phase, which has affected whole of Tibet and the northernmost part of the Himalaya. These grabens are distributed mainly along the crest of the Himalaya, southern Tibet and central Tibet (Fig. 1). In the Himalaya all the grabens are limited south of the Indus-Tsangpo Suture Zone (ITSZ) except Yadong graben, which extends up to Gulu rift. Molnar & Tapponnier (1978) firstly documented remarkably uniform spacing for north-south trending graben in southern Tibet. Armijo *et al.* (1986) reported decrease in graben spacing from south to north across the Tibetan plateau. Recently, Yin (2000) extensively documented the spacing of grabens (equivalent of rift as used by Yin 2000). He defined the graben spacing as a distance between two centers of nearby graben's basin measured perpendicular to the strike of graben. Using above definition, four distinctive zones are recognized (Fig. 1): (1) the Himalayan region (south of ITSZ) (2) the southern Tibet region (between ITSZ and Bangong-Nujiang suture) (3) the central Tibetan region (between Bangong-Nujiang suture and Jinsha suture) (4) the northern Tibetan region (north of the Jinsha suture). Graben spacing in the Himalaya and Tibet decreases systematically from south to north. It is 191±67 km in Himalaya, 146±34 km in southern Tibet and 101±31 km in

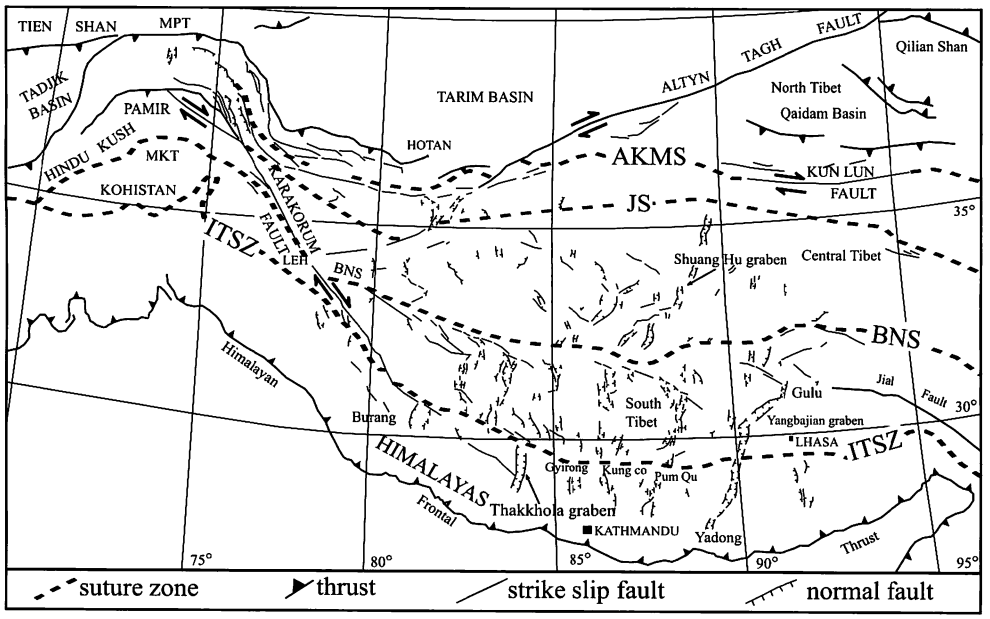

Fig. 1. Tectonic setting of the Himalaya-Tibetan orogen showing major grabens (modified after Blisniuk *et al.* 2001). AKMS: Ayimaqin-Kunlun-Mutztagh suture; BNS, Bangong Nujiang Suture; ITSZ: Indus-Tsangpo Suture Zone; JS: Jinsha Suture; MKT: Main Karakoram Thrust; MPT: Main Pamir Thrust.

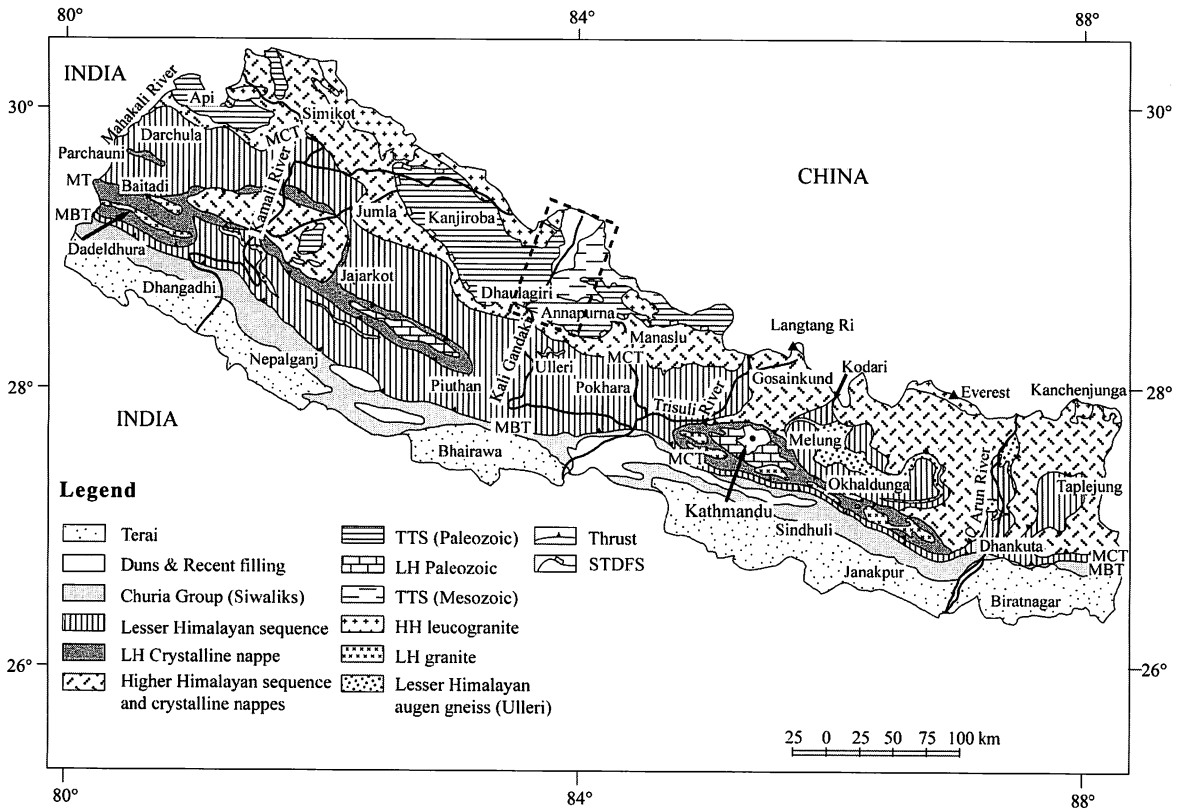

Fig. 2. Geological map of Nepal (modified after Upreti & Le Fort 1999). LH: Lesser Himalaya, HH: Higher Himalaya, TTS: Tibetan-Tethys sediments, MBT: Main Boundary Thrust, MCT: Main Central Thrust, MFT: Main Frontal Thrust, STDFS: South Tibetan Detachment Fault System. Dotted rectangle shows the location of the Thakkhola half graben.

central Tibet. The widely spaced grabens in the Himalaya and Tibet may have been related to the presence of a relatively light crust and a strong mantle lithosphere throughout the Tibet (Yin 2000). Systematic decrease in graben spacing can also be attributed to the northward decrease in crustal thickness.

GEOLOGIC SETTING OF THE THAKKHOLA HALF GRABEN

Thakkhola half graben lies in Palaeozoic to Cretaceous rocks of the Tethyan Series between STDF system (Burchfiel *et al.* 1992) to the south and ITSZ to the north (Fig. 3). It can be taken as a part of the normal fault system affecting the whole Tibetan Plateau (Molnar & Tapponier 1978), which shares uniqueness in several aspects particularly its close proximity to the Himalayan Range, to the south of the ITSZ and above the STDF. The half graben is bounded by Dolpo-Mugu-Mustang middle Miocene leucogranite (Le Fort 1975) to the west and Paleozoic and Mesozoic sediments and the Manaslu leucogranite (Le Fort 1981) in the east.

The tectonic stratigraphy of the Thakkhola half graben can be described by two different units i.e. basement and syntectonic deposits. The Tibetan Tethys sediments serve as basement whereas the half-graben basin filled by lacustrine and fluvial sediment represents the syntectonic deposits. A well-preserved Tibetan Tethys sediments are exposed in the Kali Gandaki valley (Fig. 3). In this section, nearly continuous 10 km thick succession is visible, ranging from Cambrian to early Cretaceous. The Paleozoic succession is characterized by a calcareous series, mainly comprising massive limestone and calcareous shale and local dolomitic and quartzitic horizons. The Mesozoic stratigraphy is essentially composed of Triassic calcareous shale grading upwards to Jurassic fossiliferous limestone, black shale, which are capped by the detrital units (conglomerates, sandstones) of the Early Cretaceous Chukh Group (Bordet *et al.* 1971 quoted in Godin 2003).

The syntectonic deposit of the Thakkhola half graben is composed of thick accumulation of continental debris extended over 90 km from north to south and about 20-30 km from east to west (Colchen 1999). The basin fills mollase: the Tetang and Thakkhola formations are separated by an angular unconformity. They lie on the high strain zone of the deformed Tibetan Tethys sediments. The Tetang Formation is well exposed in the southern, southeastern, and eastern parts of the basin and is composed of pebble and gravel consisting of clasts of quartzite and limestone derived from the Mesozoic bedrock, which is followed by polygenic conglomerates

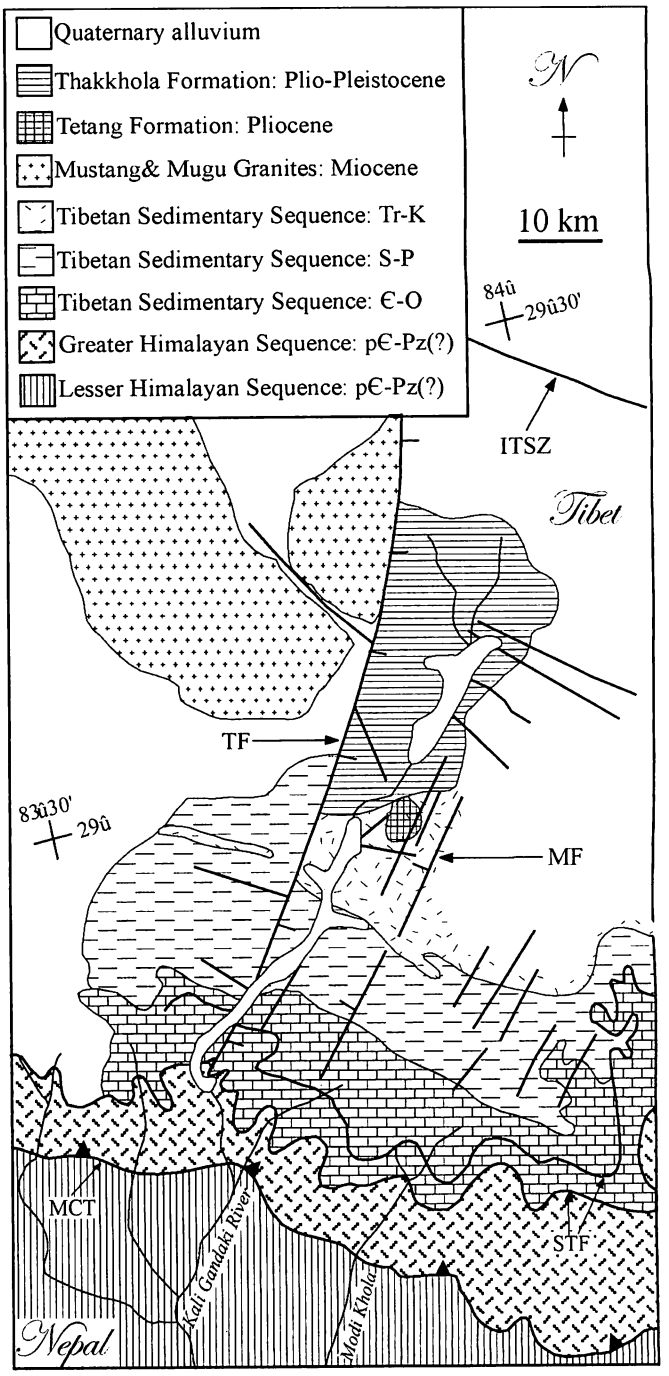

Fig. 3. Geological map of the Thakkhola and adjacent area (modified after Hurtado *et al.* 2001) MCT: Main Central Thrust, STF: normal faults of STDF system, MF: Muktinath Fault, TF: Thakkhola Fault, ITSZ: Indus Tsanpgo Suture Zone.

composed mainly of leucogranitic pebbles from Mustang leucogranites in the east. Pliocene age has been assigned for the Tetang Formation, palynologically (Fort *et al.* 1982) and magnetostratigraphically (Yoshida *et al.* 1984). The Thakkhola

Formation crops out in the western and eastern part of the Tetang Formation (Fig. 3). It comprises of conglomerates (mainly clasts of metamorphosed Paleozoic rocks) and Mustang leucogranites and is capped by alternate zones of various facies, lenses of sandstone, imbrication of polygenic conglomerates and lacustrine limestone (Colchen 1999). Magnetostratigraphic data constrain 2.48 Ma for the Thakkhola Formation (Yoshida *et al.* 1984).

Structural Setting of the Thakkhola Half Graben

The structural setting of the Thakkhola half graben bears the complex kinematic and geometrical relationship with the STDF and the Thakkhola Fault (Dangardzong Fault of Hurtado *et al.* 2001). According to Hurtado *et al.* (2001), the Thakkhola Fault was developed during Miocene, synchronous with the motion of the Annapurna detachment (a normal fault of the STDF system). The clockwise rotation and scissors-like kinematics of the Thakkhola Fault are responsible for the development of the half garben. The structural pattern of the graben is mainly controlled by a series of transverse faults (Thakkhola fault system) and cleavage striking N20°-40°, which are responsible for the asymmetric nature of the graben (Colchen 1999). The Thakkhola fault system consists of a number of extensional faults extending over several kilometers and can distinctly be observed in the west of the basin. The predominance of the sinistral Thakkhola Fault (Hurtado *et al.* 2001) has also caused remarkable asymmetry in the graben (Figs. 3 and 4). The Paleozoic-Mesozoic sequence has intensely crushed and shattered along the fault surface. These structures are accompanied by other faults which strike N180°, N115°, and N115°-160°. The syntectonic deposit is tilted where it is in direct contact with the fault. The Thakkhola Formation is characterized by NW-SE fold in the central part of the basin. On the basis of the field geological data, Thakkhola half graben cannot be considered as a true rift (e.g. Yin 2000) because there is no magmatic signature within the graben basin.

MODELLING OF THE HALF GRABEN

A number of simulations (e.g. Bott 1997; Melosh & Williams 1989; Schultz-Ela 2002) were performed to study the half graben evolution in crustal rocks. These studies were mainly focused on mechanism of graben formation and factors controlling the width and depth of a graben. In the present study, a two-dimensional plane-strain elastic finite element method is applied to simulate the stress field and faulting in the Thakkhola half graben. The plane strain assumption is justified because grabens are generally much longer than their width. Although surface processes are also important to control tectonic processes, we do not consider these in modelling. Results of the numerical simulations largely depend on the several rock layer properties, geometries and boundary conditions. Since the rock layer properties of the upper crust are relatively well known, the poorly unknown parameters are constrained to the limited range so that simulated models reveal the realistic results. Therefore, the modelling not only shows the stress field and resulting faults but also predicts probable values for the rock layer properties controlling the half-graben evolution.

Model Set Up and Boundary Conditions

To simulate the half graben, the cross-section (Fig. 5) given by Colchen (1999) was chosen and simplified according to similarity of the rock layer properties. The model cross-section is 56 km long and the thickness varies up to 12 km representing the overall structural configuration of the half graben. Two types of geometry have been considered, with and without detachment fault (Thakkhola Fault). Since it is impossible to allow slip along the fault plane in the proposed model, we will consider the detachment fault and STDF as a weak zone. Structural data of the region have revealed that the Thakkhola Fault merges with the STDF system décollement at depth with a listric-geometry (Fig. 4) (Hurtado *et al.* 2001).

In order to simulate the natural situation, we impose simple but reasonable boundary conditions representing the present day kinematics in the southern Tibet. In both the models, the upper surface was free and the lower boundary was only permitted to deform horizontally. The nodes along the left boundary of each model can only move vertically whereas from the right side of the models, we impose extensional displacement progressively from 10 m to 50 m at the rate of ~ 1 mm/year (Jouanne *et al.* 2004) to produce horizontal extension (Fig. 6). Based on Yin's (2000) model we also imposed spreading boundary condition, which is not shown here.

Rock Layer Properties

Results of the numerical modelling strongly depend on several rock layer properties, geometries and boundary conditions. Therefore several rock layer properties were varied systematically to understand their effect on the structural evolution of the Thakkhola half graben. For the sake of simplicity in calculation, the entire model is divided into two layers excluding weak detachment zone taking account of stratigraphy and mechanical properties of the rock types therein. Each layer has been assigned with distinct rock layer properties providing emphasis on the dominant rock type. We perform parametric calculation using different values of key parameters, e.g. density, Young's modulus, cohesion and

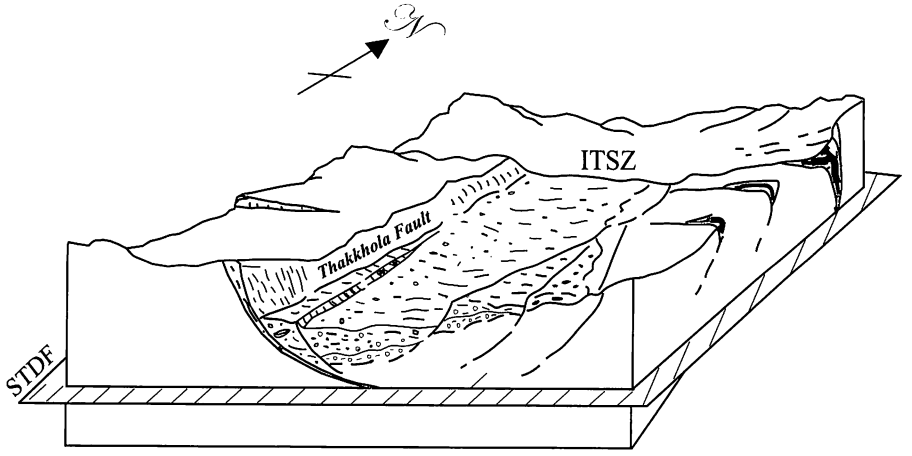

Fig. 4. Structural disposition of the Thakkhola half graben (modified after Colchen 1999). STDF: South Tibetan Detachment Fault system, ITSZ: Indus Tsangpo Suture Zone.

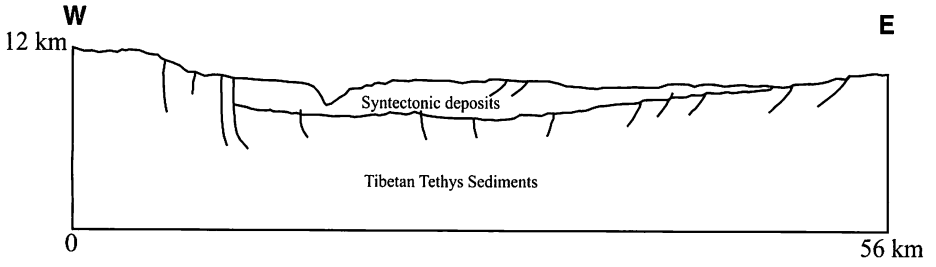

Fig. 5. E-W structural cross section of the Thakkhola half graben (modified after Colchen 1999).

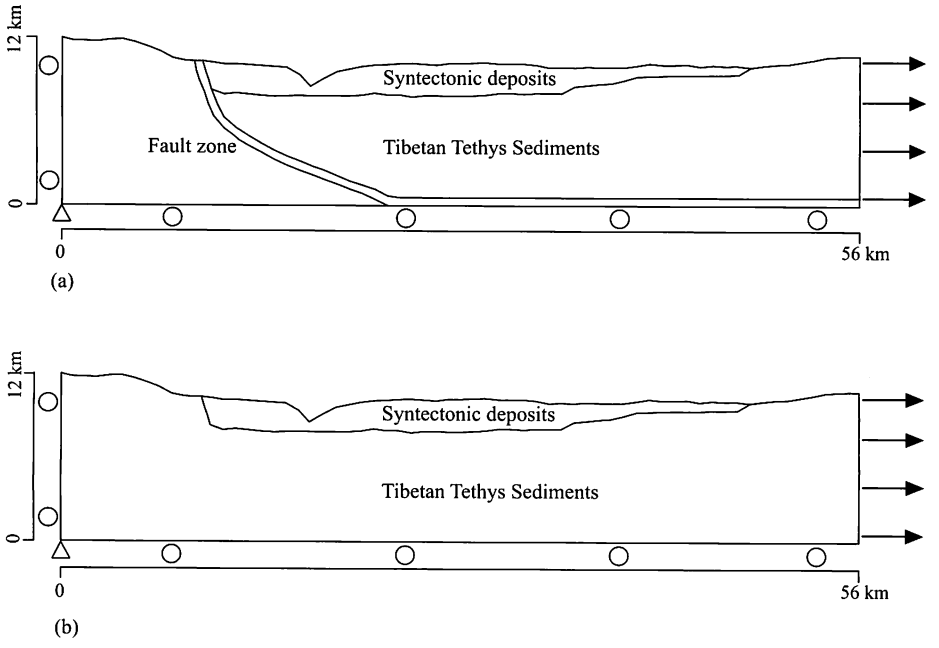

Fig. 6. Geometry and boundary condition of the model. **(a)** with detachment fault **(b)** without detachment fault.

Table 1. *Rock layer properties.*

Layer	Lithology	Density (kg/m^3)	Young's modulus (GPa)	Poisson ratio	Cohesion (MPa)	Friction angle (degree)
TTS	limestone, shale, sandstone	2670	40	0.25	30	41
syntectonic deposit	conglomerate, siltstone, glacio-lacustrine sediments	2140	22	0.25	18	30
fault (weak zone)	crushed rock	2670	1	0.25	9	20

friction angle (Fig. 7). We adopt the most suitable set of layer properties for calculation, as shown in Table 1.

MODELLING RESULTS

Primarily based on the geologic cross-section (Colchen 1999), the stress regime of the Thakkhola half graben was simulated. Since our model consists of two types of geometries (with or without detachment fault), the simulated stress regimes are explained with respect to both model geometries. The gravitational force is taken into account and horizontal extension is applied progressively. Since the result of spreading boundary condition is not consistent with nature, we do not show models with that boundary condition.

Stress Field

In the first model, we assume detachment fault as a weak zone. This zone resembles Thakkhola fault system in nature. Since our model cannot simulate the slip on the fault, this assumption bears some meaning in this regard. The rock layer properties for this zone are assigned in such a way so that it could simulate the slip along the detachment. The stress field under 10 m horizontal extension is shown in Fig. 8a. Compressive nature of the stress was found in all layers. The lower magnitude of σ_1 and σ_3 was observed in upper part of the model. The orientation of σ_1 and σ_3 was vertical and horizontal respectively. With increasing horizontal extension, a tensional stress (indicated by red lines in stress field in all models) was induced in the upper part of both layers (Fig. 8b). Such stress field can induce normal faulting in extensional regimes.

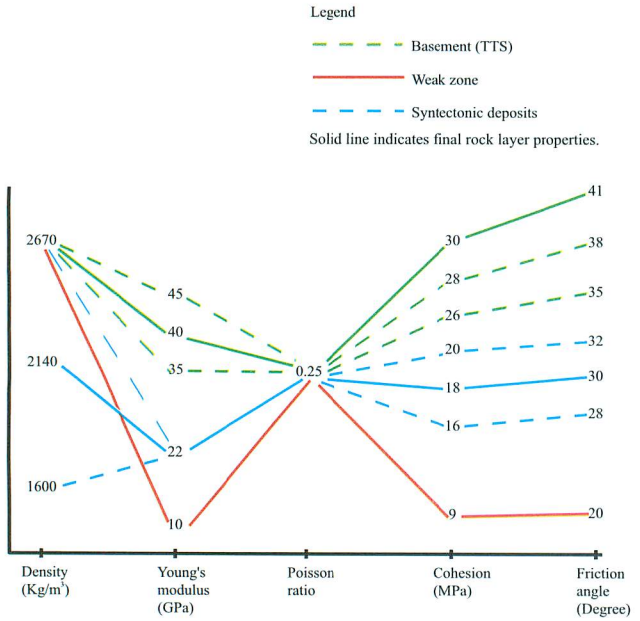

Fig. 7. Chart showing the variation of rock layer properties during computation.

No significant differences were observed the stress state and magnitude in the model without detachment fault. At the initial stage of extension, mostly compressive state of stress was observed (Fig. 9a). During progressive increase in extension, a tensional stress field was dominantly observed in the upper part of both layers (Fig. 9b), to produce normal faulting. No significant changes were observed in the stress field though density contrast was applied.

Pattern of Mohr-Coloumb Failure

The failure pattern was simulated using Mohr-Coloumb criterion (Melosh & William 1989). In this study one of the interests was to investigate effect of the detachment fault on development of the Thakkhola half graben. It is reasonable to describe failure pattern separately for two different cases, with and without detachment fault.

Models with detachment fault

At the initial extension of 10 m both layers were free from failure elements. At 20 m extension faults are developed only in basement rock near the weak zone. However no faults occurred within the hanging wall block (Fig. 10a). With the increasing extensional displacement, failure elements were observed around the weak zone in the basement. Some failure elements are localized on either side of the gorges of the Kali Gandaki River and these might be the effect of model geometry (Fig. 10b). With 40 m extensional displacement, failure elements emerged in the upper part of the basement and western part of

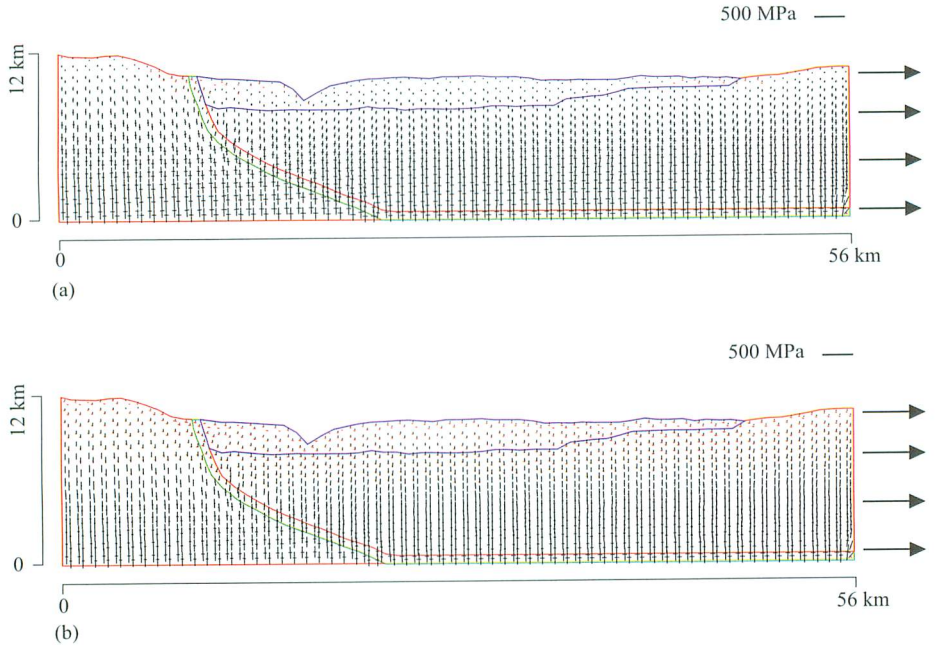

Fig. 8. Stress field at **(a)** 10 m **(b)** 50 m horizontal extension with detachment fault. Every pair of perpendicular lines represents σ_1 (long lines) σ_3 (short lines) in stress field. Red lines show tensional stress field.

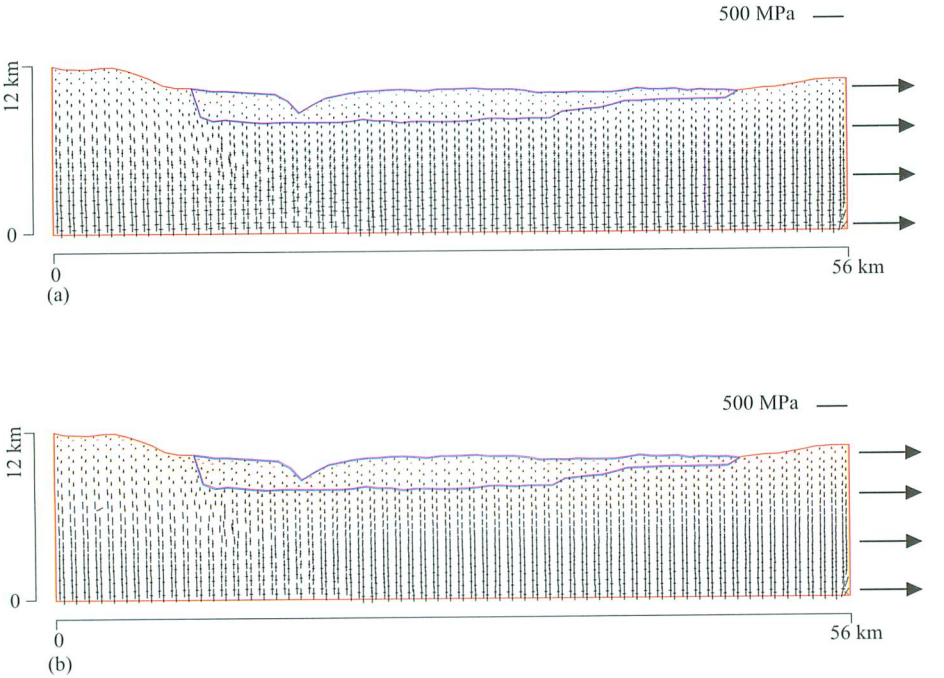

Fig. 9. Stress field at **(a)** 10 m **(b)** 50 m horizontal extension without detachment fault. Every pair of perpendicular lines represents σ_1 (long lines) σ_3 (short lines) in stress field. Red lines show tensional stress field.

the syntectonic deposits (Fig. 10c). These failure elements correspond to the graben bounding faults. As the applied extension is progressively increased, failure elements both in tension and compression extend into the deeper part. At 50 m extensional displacement failure elements were extensively developed in both layers (Fig. 10d). A notable difference was observed on failure pattern during the density variation of the syntectonic deposits as more elements were failed in the basement with increasing density (Fig. 11a). Conversely, decreasing density resulted few failure elements in the basement (Fig. 11c). The overall pattern of failure elements replicates the nature.

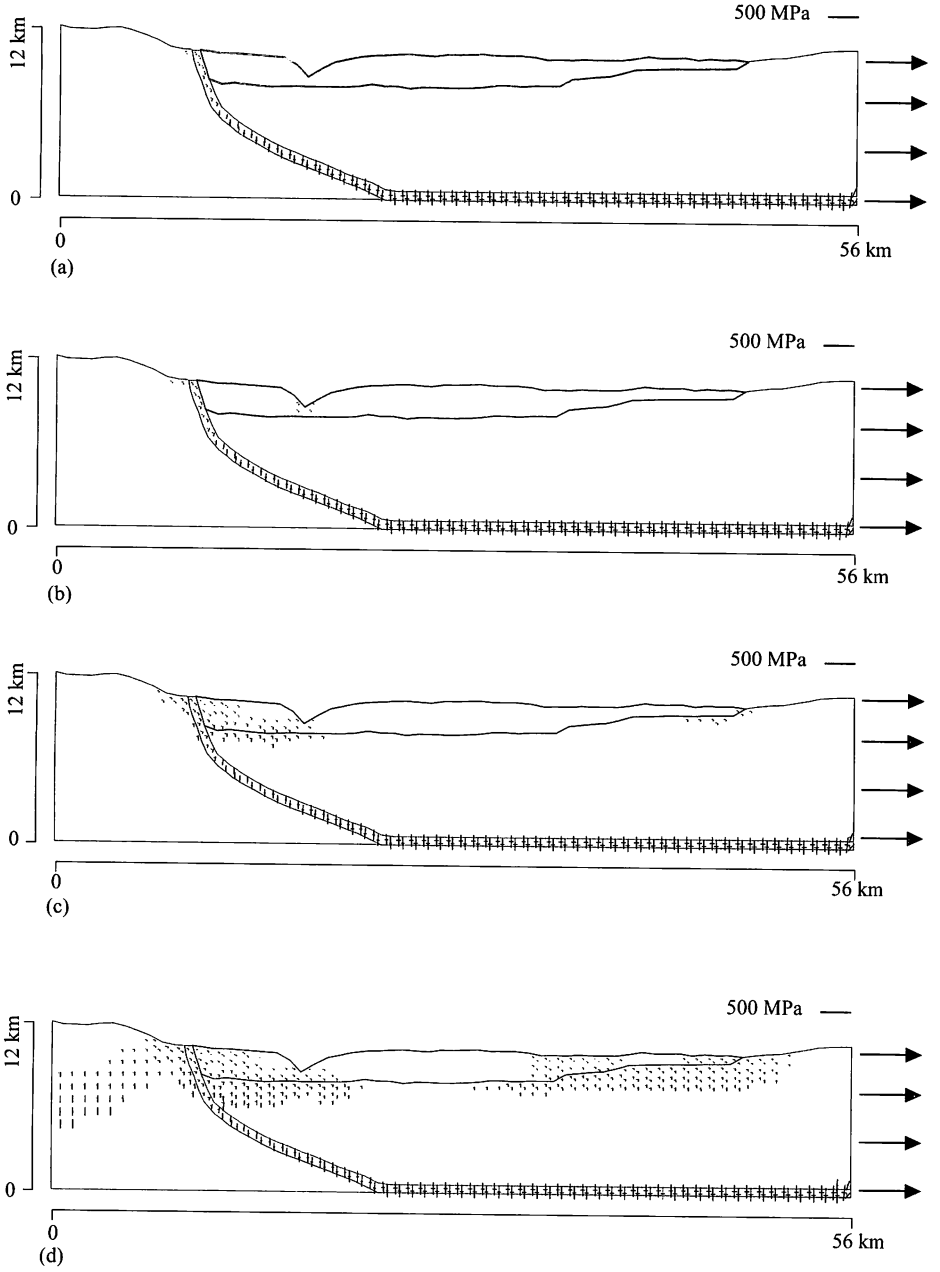

Fig. 10. Failure elements at **(a)** 20 m **(b)** 30 m **(c)** 40 m **(d)** 50 m horizontal extension with detachment fault. Every pair of perpendicular lines represents σ_1 (long lines) σ_3 (short lines) in failure element. Red lines show tensional stress field.

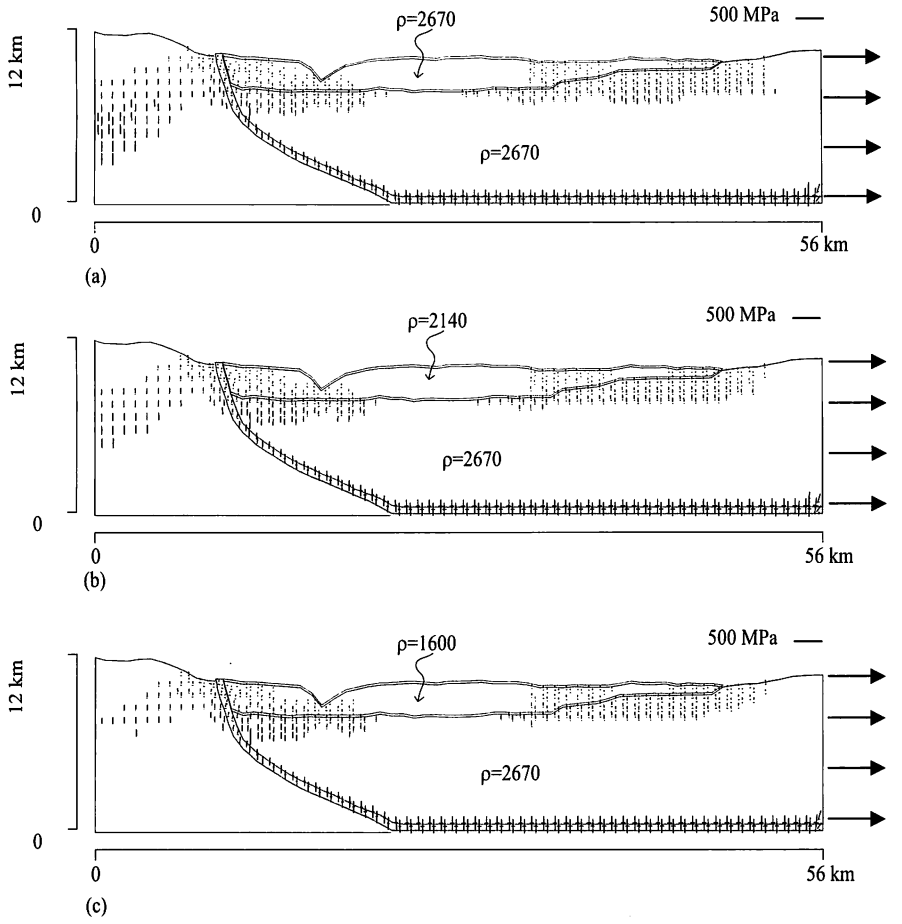

Fig. 11. Failure elements at 50 m horizontal extension with detachment fault (**a**) increasing density (**b**) standard value (**c**) decreasing density of the syntectonic deposits. Every pair of perpendicular lines represents σ_1 (long lines) σ_3 (short lines) in failure element. Red lines show tensional stress field.

Models without detachment fault

As we aimed to understand the effect of the detachment fault on half graben evolution, we also simulate failure elements for this case. Our model did not show any failure until 20 m extensional displacement. At 30 m extension few elements were failed around gorges of the Kali Gandaki River. As the applied extension is increased the failure elements are localized on the top of the basement and western part of the syntectonic deposits (Fig. 12a). Increasing extension failure elements are extensively developed in both layers (Fig. 12b). Overall results merely differ to that of model with detachment fault. In contrast to the model with detachment fault, increase in density of syntectonic deposits, few elements were failed in the basement (Fig. 13a). Conversely, decreasing density failure elements are developed beyond the graben bounding faults, which are deeply rooted and cannot precisely replicate the nature (Fig. 13c). This indicates that the initial fault together with rock layer properties has significant effect on the depth of the fault, which consequently influences the width of the graben.

DISCUSSION

Model Set-Up

The finite element models, presented and discussed above, have been performed in two-dimensional space, with a simple present-day geometry of the Thakkhola half graben assuming homogeneous and isotropic material within the individual layer. Furthermore, the rock layer properties used in the simulation were not experimentally determined. We performed a series of test calculations using different values of key parameters. Finally, we adopted only the most suitable set of rock layer properties for calculation. Further, we assumed that the crust behaves elastically though it is brittle-elastic-plastic in nature.

Stress State in the Himalaya-Tibet Orogen

A large numbers of authors have made attempts to assess the state of stress in the Himalaya and adjacent areas (e.g.

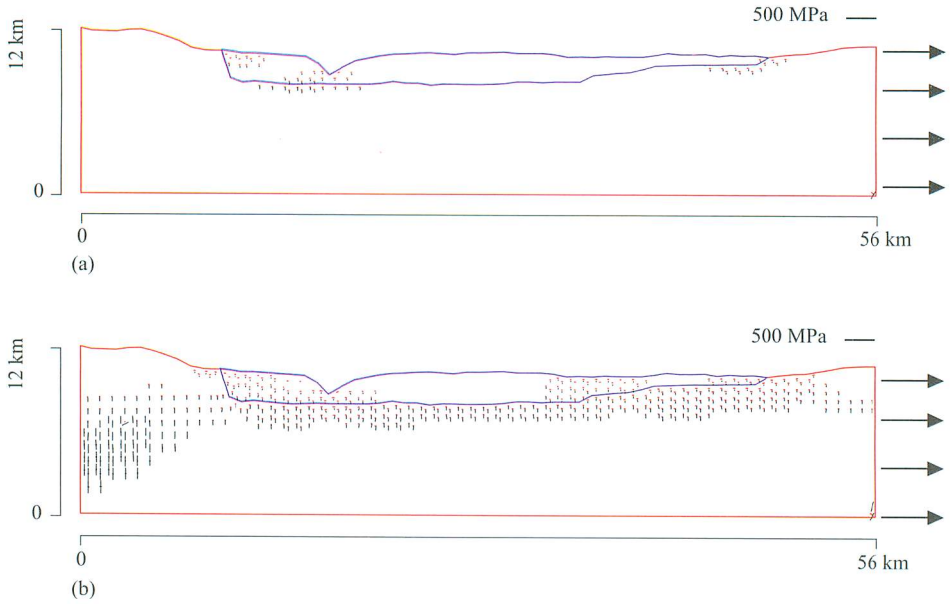

Fig. 12. Failure elements at (**a**) 40 m (**b**) 50 m horizontal extension without detachment fault. Every pair of perpendicular lines represents σ_1 (long lines) σ_3 (short lines) in failure element. Red lines show tensional stress field.

Cloetingh & Wortel 1986; Shanker *et al.* 2002, Chamlagain & Hayashi 2004, 2006). Nakata *et al.* (1990) deduced the N-S direction of the maximum horizontal principal stress (σ_{Hmax}) for eastern and central sectors of the Himalaya using the geometry and orientation of the active faults. They further noted that the direction of σ_{Hmax} have changed following a change in the direction of the relative motion between the Indian plate and the tectonic sliver which has detached together along the transcurrent faults in the Eurasian Plate. These studies clearly indicate that regional direction of σ_{Hmax} is consistent with relative plate motions at least in the central sectors of the Himalaya. The stress state in the northern most part of the Himalaya and Tibet is quite different due to different tectonic regimes and structural configuration. Immediately north of the highest peak of the Himalaya, the tectonic regime is dominated by east-west extension, which is dominantly characterized by strike slip and normal fault systems (Blisniuk *et al.* 2001). Further, fault plane solutions of the central Tibet indicate large components of normal faulting under extensional stress regime (Molnar & Tapponier 1978). The kinematics drawn from microtectonic measurements has also revealed the similar state of stress in the southern Tibet (Tapponier *et al.* 1981).

Paleostress analysis (Colchen 1999) in the Thakkhola basin has successfully shown polyphased faulting and stress direction with relative chronology: (a) N-S compressional stress regime with dextral and sinistral conjugate strike slip faults (b) extensional regime with recurrence of strike slip faults in normal faults 14 Ma ago (Coleman & Hodges 1995) (c) extensional regime during Tetang and Thakkhola periods (Pliocene probably to Pleistocene). The proposed numerical models also show the tensional nature of the stresses in the upper part of the models. The lower part of the models is characterized by higher magnitude of the compressive stresses. In an extensional regime, the maximum principal stress (σ_1) is vertical whereas minimum stress (σ_3) is horizontal (Anderson 1951). Since the orientation of σ_1 and σ_3 stresses is vertical and horizontal respectively, the applied boundary condition is suitable for simulating extensional fault system. With increasing horizontal extensional displacement, tensional stress is dominantly observed in the upper part of both layers. This stress field is in good agreement with the stress field derived from the paleostress analysis. Changes in horizontal extension do not affect the stress distribution pattern throughout the simulation.

Development of Graben Faults in the Thakkhola Half Graben

The Thakkhola half graben is bounded by two major normal faults; Thakkhola Fault in west and Muktinath Fault in the east. These faults extend up to ITSZ to the north and STDF to the south. Thakkhola Fault has caused significant asymmetry in the graben and merges to STDF décollement at depth with a listric geometry. Apart from these, numerous submeridional faults with both synthetic and antithetic nature have been

mapped both in the syntectonic deposits and basement rock. In the models, extensional graben faults formed at the top of the overburden and propagated downward. At the initial stage of extension, faulting mainly occurred on eastern and western side of the models, and these correspond with the major graben bounding faults. The proposed models suggest that natural grabens have multiple faults on each side rather than single fault and can be realized in the model where diffused failure elements are observed. The spacing between these failure zones clearly replicates the graben width. However failure elements in the western sector of the model is deeper than the eastern sector, which is characteristic of the development of the half graben. In this regard this simulation gives insights to the first order characteristics of the Thakkhola half graben development. The models also lead to conclusion that the structural development of the half graben depends sensitively on the rock layer properties. Assumption of a weak zone does not make significant difference on stress distribution except faulting. Thus it seems that the weak zone (equivalent to the Thakkhola Fault system) did not contribute significantly to the development of the half graben. Instead topographical loading and tectonic boundary conditions might have played an important role.

Factors Controlling Graben Dimensions

Despite numerous researches, factors controlling graben dimensions have not been completely understood. A large number of factors (e.g. rheology, depth of initial fault) may have significant influence on graben width. Golombeck (1979) pointed out the effect of layer discontinuity in material properties but it is not always true that the initial fault will always terminate in such a rheological discontinuity. In some situations plane of weakness, local inhomogeneties, or stress concentrations may be effective factors. Melosh & Williams (1989) showed that the depth of initial normal fault primarily control the width of the graben rather than depth of the mechanical layer discontinuity. In this study we found that density of the syntectonic deposit is an important factor to induce failure element at different depths. The model with detachment fault showed consistent results where depth of failure elements increases with increasing density (Fig. 11). Further failure elements occupied wider area. However reverse effect was observed in the models without initial detachment fault (Fig. 13). These results indicate that high density syntectonic deposits may facilitate development of greater widths and limiting depths of the half graben. This is consistent with the Bott's (1997) results where he found reduction in width of the half graben and amount of subsidence with lowering the density of syntectonic deposits. However the effect of stress state in the brittle crust cannot be ruled out as proposed by Reiter *et al.* (1992).

Seismicity Around the Thakkhola Half Graben

The entire territory of Nepal is characterized by intense microseismic activity but lateral variations are also observed. The microseismic activity is particularly active in eastern and far-western Nepal with small clustering in central Nepal Himalaya. A detailed study of microseismic events reveals three distinct clusters i.e. in eastern Nepal it lies between longitudes 86.5°E and 88.5°E, central Nepal 82.5°E and 86.5°E (south east of the Thakkhola half graben) and western Nepal 80.5°E and 82.5°E (Fig. 14).

The seismicity in southern Tibet is quite different. It has experienced a number of deep-seated mantle normal fault earthquakes sporadically (Chen & Kao 1996). Mostly microseismic events tend to be localized near the main active N-S normal fault in southern Tibet. Microseismic data show the intense and continuous activity along the Pum Qu graben. Thakkhola and Kung Co grabens show continuous moderate seismicity (Fig. 14). It is therefore clear that most of the microseismic events are concentrated along the N-S grabens and active normal fault of the southern Tibet. Further, higher critical cohesive strength (Mandl & Shippam 1981; Appendix) around the graben bounding faults (Fig. 15) corresponds to high seismicity zone (Fig. 14) of the Thakkhola half graben. Thus it can be inferred that the graben bounding faults are still active and can contribute to east-west extensional tectonics in the Himalaya-Tibet region.

Proposed Mechanism for Genesis of the Thakkhola Half Graben

Despite numerous researches, there is still debate on graben evolution and east-west extension in the Himalaya-Tibet orogen. In this context the gravitational collapse driven by the excess gravitational potential energy can simply explain the viable mechanism for this most debated topic. Yin (2000) proposed a general model for all Himalaya-Tibet rifts giving emphasis on the asthenospheric upwelling beneath the Himalaya and Tibet. According to the model, the upper crustal normal faults sole into the ductile shear zone in the middle and the lower crust. The mantle lithosphere is thinned in response to extension either by brittle faulting in the upper crust or ductile flows in the lower crust. Because of lithospheric thinning, the mantle asthenosphere is upwelled and produced synrifting magmatism in the rift valley. This model can explain the origin of the Baikal rift and Shanxi graben in the southeast Siberia, and the north China. In contrast there is no evidence of magmatism in the Thakkhola half graben. Further we

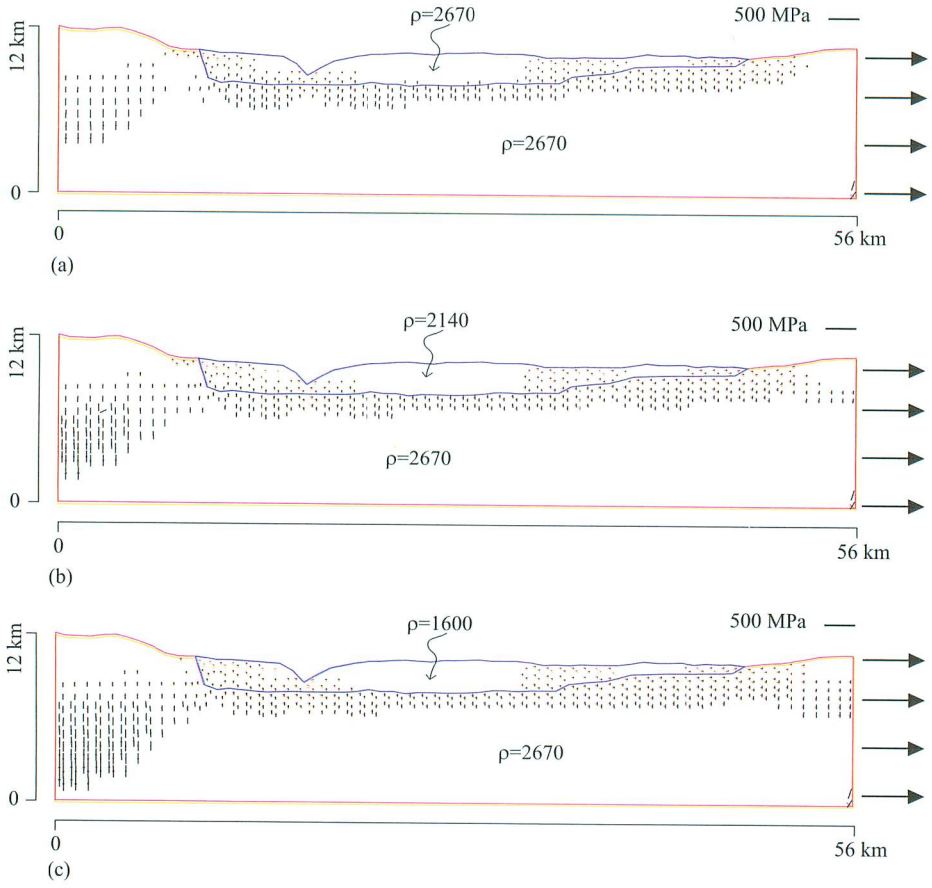

Fig. 13. Failure elements at 50 m horizontal extension without detachment fault **(a)** increasing density **(b)** standard value **(c)** decreasing density of the syntectonic deposits. Every pair of perpendicular lines represents σ_1 (long lines) σ_3 (short lines) in failure element. Red lines show tensional stress field.

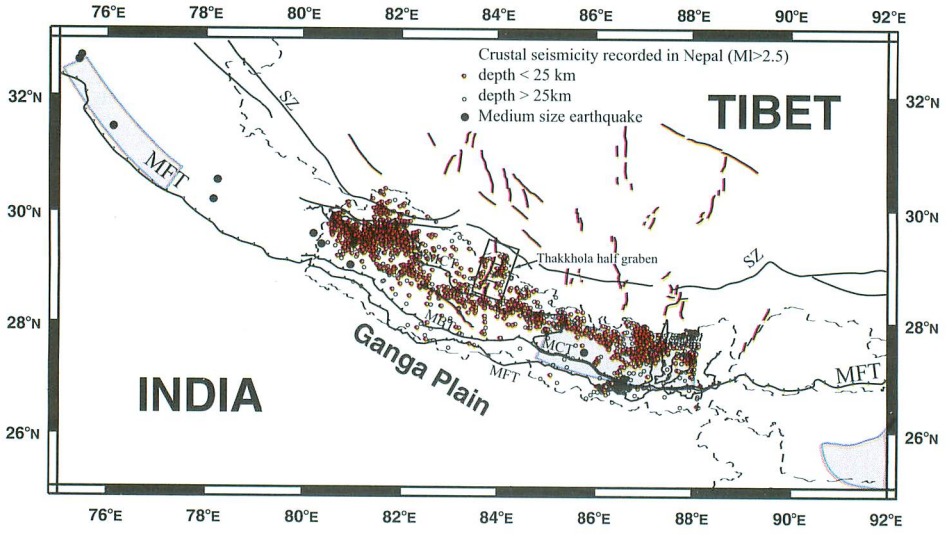

Fig. 14. Seismicity in Nepal (after Jouanne *et al.* 2004). The intense microseismicity drawn with small grey circles, tend to cluster south of the Higher Himalaya at a mid-crustal level. Star represents medium size earthquake.

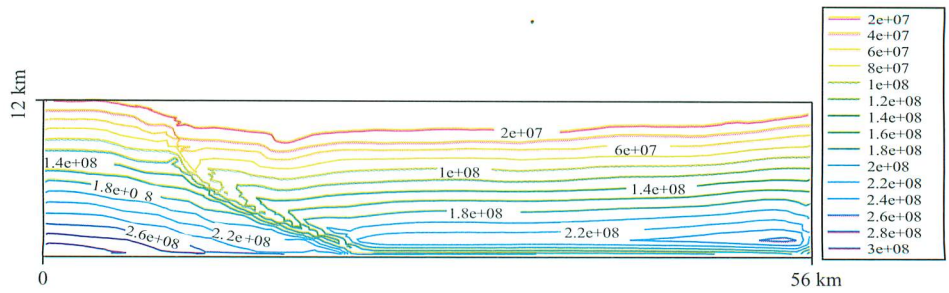

Fig. 15. Critical cohesive strength (in Pa) with detachment fault at 50 m horizontal extenson.

imposed boundary condition in accordance with the Yin's model, but the simulated results did not resemble with the nature. Thus Yin's (2000) model can be ruled out. Recently, using plasticine models, Dubey & Bhakuni (2004) showed the simultaneous development of normal faults (N-S trending) in the hanging wall and strike slip faults in the footwall of the Tethyan fault. This structural development has been attributed to the effect of the frontal and oblique ramp geometries and explains the extensional tectonics of the Himachal Himalaya in the western Himalaya. However they did not consider gravity in their model. Since they gave emphasis on the elevation, it is necessary to quantify the elevation from the scaled model to compared with nature. If we consider elevation, the altitude of the Thakkhola half graben ranges from 3000-4000 m (Colchen 1999), which is too small as compared to their modelling. Furthermore, it was formed at lower elevation than it shows at present. Therefore their model is not consistent with the formation of the Thakkhola half graben in the central Nepal Himalaya and can be applied where frontal and oblique fault ramps are present and not for the grabens of the entire Himalaya-Tibet region.

It is suggested that the Tibetan plateau uplift and east-west extension are responsible for the Thakkhola half graben evolution. The most debated point is timing of the plateau uplift and east-west extension. Garzione *et al.* (2000) argued that the Tibetan Plateau attained its current elevation prior to the east-west extension using isotopic composition of meteoric water ($\delta^{18}O$). Further, they reported that the initiation of the Thakkhola half graben extension is constrained between 10 and 11 Ma based on magnetostratigraphy of the older Tetang Formation. Based on the available field information and our modeling results, we proposed a schematic model (Fig. 16). Since the onset of subduction, the Indian Plate deformed in different stages. According to Chemenda *et al.* (2000) subduction of the Indian Plate caused the formation of huge accretionary prism and failure of the subducted crust (Fig. 16a). After the first break-off (Fig. 16b), delamination occurred by which Indian upper crust started to underplate with Eurasian lithospheric mantle (Fig. 16c). This caused the onset of uplift in Tibet. After the second break-off, the whole regime switched to compressional state and the MCT was formed around 24 Ma (Fig. 16d). It is believed that STDF was formed coeval with the MCT at this stage. Because of buoyancy, crustal flow occurred beneath Tibet by which Eurasian lithospheric mantle was replaced by the Indian upper continental crust (Fig. 16e). This major event around 14.5 Ma (Coleman & Hodges 1995) caused significant uplift in Tibet and it attained the maximum elevation. In this stage topography related excess gravitational potential energy (GPE) of the Himalayan-Tibetan Plateau relative to the surrounding lowland area exceeds the compressional stresses related to the continent-continent collision, which caused the east-west extension in the Himalayan-Tibetan orogen (Fig. 16f). The excess ΔGPE can be calculated by

$$\Delta GPE = \int_{-h}^{z} \Delta\rho g z dz$$

where h is the elevation of the plateau above the reference lowland, z is the depth, $\Delta\rho$ is the density contrast between the plateau and lowland at depth z, and g is the acceleration due to gravity. The geochronological data have also shown that this event occurred after plateau attained its maximum elevation (Coleman & Hodges 1995; Garzione *et al.* 2000). This major extensional phase was solely responsible for the initiation of the Thakkhola half graben in the crest of the Himalaya. After the initiation of the Thakkhola Fault, hanging wall block in response to extension subsided isostatically. For the mechanism to be effective, low velocity zone (partially molten) beneath the Himalaya-Tibet might have allowed ductile flow of the lower crust. Further extension in the graben might have caused due to movement along the Karakoram fault and STDF. Hurtado *et al.* (2001) argued that the Dangardzong fault (equivalent to the Thakkhola Fault) and its kinematics with the Annapurna detachment (normal fault of the STDF) played crucial role during its development. Our numerical models, however merely revealed difference between model with or without detachment fault in development of the half graben. Instead, rock layer properties are found to be sensitive to the graben evolution. Although numerous factors might have

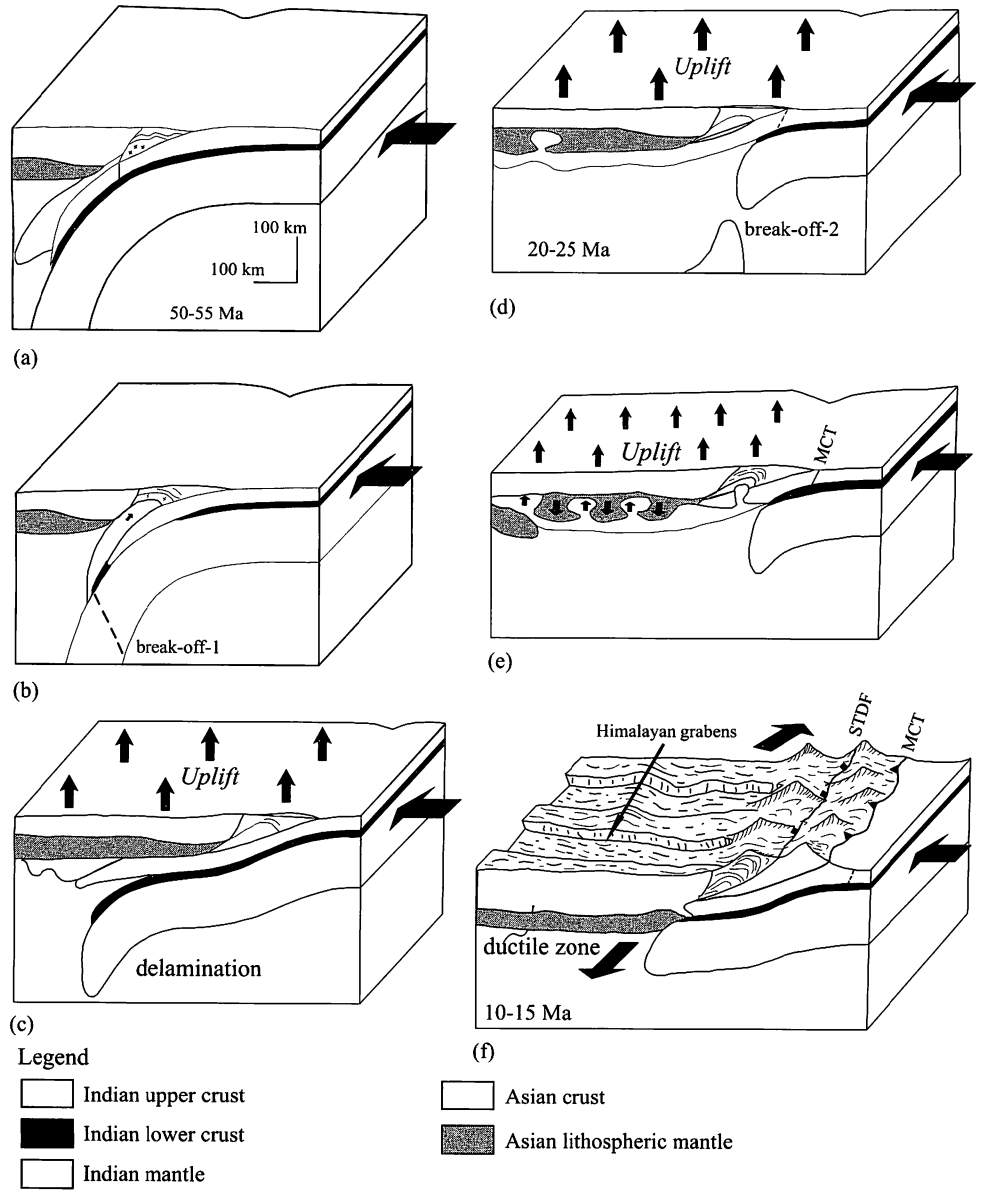

Fig. 16. Schematic model showing the tectonic evolution of the Himalayan grabens.

contributed to the formation of north-south trending graben, their relative roles are often debated. However the extension caused by topographical loading and its excess gravitational potential energy could be the major factors. Admittedly, role of basal shear, rheologic structure and tectonic boundary condition cannot be ignored.

CONCLUSIONS

The N-S trending grabens in southern Tibet and crest of the Himalaya probably formed due to gravitational collapse driven by excess gravitational potential energy built up by continuous subduction of the Indian Plate beneath the Himalaya-Tibetan orogen. A series of numerical models are presented for the Thakkhola half graben, which is one example of the extensional tectonic events in the Himalaya. Our models are able to simulate reasonable stress field that corresponds to the paleostress analysis. The simulated models show that the extensional graben faults form at the overburden and propagate downward as the extension is progressively increased. Consequently, failure elements are clustered at two extremities of the graben, which directly correspond to the graben bounding faults. Our results suggest that natural grabens have multiple faults on each side rather than a single

fault. These faults, however, initiate nearly at the same time, but not exactly, simultaneously. Further their depth increases with the applied extension. Syntectonic deposits characterized by normal faulting in a tensional tectonic stress field, is common for small-scale grabens at post rift deformation stage. Our models also show that density of the syntectonic deposit can influence the graben fault depth, which consequently affect the dimensions of the half graben of kilometer scale. The applied rock layer properties with the proposed geometry and boundary condition are able to deduce the first order characteristics of the Thakkhola half graben. Our modelling results suggest the extension model rather than mantle upwelling with spreading model for the grabens of the Himalaya-Tibetan orogen

Acknowledgements: D.C. is grateful to the Ministry of Education, Science, Sports and Culture, Japan, for the scholarship to carry out this research. We thank Dr François Jouanne for permission to use Fig. 14.

References

Anderson, E.M. 1951. *Dynamics of Faulting.* Oliver and Boyd, Edinburg.

Armijo, R., Taponnier, P., Mercier, J.L., Han, T. 1986. Quaternary extension in the southern Tibet: Field observation and tectonic implications. *Journal of Geophysical Research,* **91**, 13803-13872.

Blisniuk, P., Hacker, B.R., Glodny, J., Ratschbacher, J., Bi, S., Wu, Z., Mcwilliams, M.O., Calvert, A. 2001. Normal faulting in Central Tibet since at least 13.5 Myr ago. *Nature,* **412**, 628-632.

Bordet, P., Colchen, M., Krummenacher, D., Le Fort, P., Mouterde, R., Remy, M. 1971. Recheerches geologiques dans l'Himalaya du Nepal:region de la Thakkhola. *Editions du center National de la Recherche Scitifique,* Paris, France, 279p.

Bott, M.H.P. 1997. Modelling the formation of a half graben using realistic upper crustal rheology. *Journal of Geophysical Research,* **102**, 24605-24617.

Burchfiel, B.C., Chen, Z., Hodges, K.V., Liu, Y., Royden, L.H., Deng, C., Xu, J. 1992. The South Tibetan Detachment System, Himalayan orogen: Extension contemporaneous with and parallel to shortening in a collisional mountain belt. *Geological Society of America, Special Paper,* **269**, 1-41.

Chamlagain, D., Hayashi, D. 2004. Numerical simulation of fault development along NE-SW Himalayan profile in Nepal. *Journal of Nepal Geological Society,* **29**, 1-11.

Chamlagain, D., Hayashi, D. 2006. Neotectonic fault analysis by 2D finite-element modelling for studying the Himalayan fold-and-thrust belt in Nepal. *Journal of Asian Earth Sciences* (In press).

Chemenda, A.I., Burg, J.P., Mattauer, M. 2000. Evolutionary model of the Himalaya-Tibet system: geopoem based on new modeling, geological and geophysical data. *Earth and Planetary Science Letters,* **174**, 397-409.

Chen, W.P., Kao, H. 1996. Seismotectonics of Asia: Some recent progress. *In*: Yin, A. & Harrison, T.M. (eds.), *The Tectonics of Asia.* Cambridge University Press, New York, 37-52.

Cloetingh, S., Wortel, R. 1986. Stress in the Indo-Australian Plate. *Tectonophysics,* **132**, 49-67.

Colchen, M. 1999. The Thakkhola-Mustang graben in Nepal and the Late Cenozoic extension in the Higher Himalayas. *Journal of Asian Earth Sciences,* **17**, 683-702.

Coleman, M.E., Hodges, K.V. 1995. Evidence for Tibetan Plateau uplift before 14 Myr ago from a new minimum age for east-west extension. *Nature,* **374**, 49-52.

Dubey, A.K., Bhakuni, S.S. 2004. Development of extension faults on the oblique thrust ramp hanging wall: example of the Tethys Himalaya. *Journal of Asian Earth Sciences,* **23**, 427-434.

England, P., Houseman, G. 1989. Extension during continental convergence, with application to the Tibetan Plateau. *Journal of Geophysical Research,* **94**, 17561-17579.

Fort, M., Freyet, P., Colchen, M. 1982. Structural and sedimentological evolution of the Thakkhola Mustang graben (Nepal Himalaya). *Zeitschrift fur Geomorphologie,* **42**, 75-98.

Garzione, C.N., Dettman, D.L., Quade, J., DeCelles, P.G., Butler, R. 2000. High times of the Tibetan Plateau: Paleoelevation of the Thakkhola graben, Nepal. *Geology,* **28**, 339-342.

Godin, L. 2003. Structural evolution of the Tethyan sedimentary sequence in the Annapurna area, central Nepal Himalaya. *Journal of Asian Earth Sciences,* **22**, 307-328.

Golombeck, M.P. 1979. Structural analysis of lunar grabens and the shallow crustal structure of the Moon. *Journal of Geophysical Research,* **84**, 4657-4666.

Hurtado Jr, J.M., Hodges, K.V., Whipple, K.X. 2001. Neotectonics of the Thakkhola graben and implications for recent activity on South Tibetan fault system in the central Nepal Himalaya. *Bulletin of the Geological Society of America,* **113**, 222-240.

Jaeger, J.C., Cook, N.G.W. 1979. *Fundamentals of rock mechanics* (3rd ed.). Chapman and Hall, London. 593p.

Jouanne, F., Mugnier, J.L., Gamond, J.F., Le Fort, P., Pandey, M.R., Bollinger, L., Flouzat, M., Avouac, J.P. 2004. Current shortening across the Himalayas of Nepal. *Geophysical Journal International,* **157**, 1-14.

Le Fort, P. 1975. Himalayas: The collided range. Present knowledge of the continental arc. *American Journal of Sciences,* **275A**, 1-44.

Le Fort, P. 1981. Manaslu leucogranite: a collision signature of the Himalaya, a model for its genesis and emplacement. *Journal of Geophysical Research,* **86**, 10545-10568.

McCaferry, R., Nabelek, J. 1998. Role of oblique convergence in the active deformation of the Himalayas and southern Tibetan Plateau. *Geology,* **26**, 691-694.

Melosh, H.J., Williams, C.A. Jr. 1989. Mechanics of graben formation in crustal rocks: A finite element analysis. *Journal of Geophysical Research,* **94**, 13961-13973.

Mandl, G., Shippam, G.K. 1981. Mechanical model of thrust sheet gliding and imbrication. *In:* McClay, K.R. & Price, N.J. (eds.), *Thrust and Nappe Tectonics.* The Geological Society of London. 79-98.

Molnar, P., Tapponier, P. 1978. Active tectonics of Tibet. *Journal of Geophysical Research,* **83,** 5361-5375.

Nakata, T., Otsuki, K., Khan, S.H. 1990. Active faults, stress field, and plate motion along the Indo-Eurasian plate boundary. *Tectonophysics,* **181**, 83-95.

Reiter, M., Baroll, M.W., Cather, S.M. 1992. Rotational buoyancy tectonics and models of simple half graben formation. *Journal of Geophysical Research,* **97**, 8917-8926.

Royden, L.H., Burchfiel, C., King, R.W., Wang, E., Chen, Z., Shen, F., Liu, Y. 1997. Surface deformation and lower crustal flow in eastern Tibet. *Science,* **276**, 788-790.

Schultz-Ela, D.D., Walsh, P. 2002. Modelling of grabens extending above evaporites in Canyonlands National Park, Utah. *Journal of Structural Geology,* **24**, 247-275.

Seeber, L., Pecher, A. 1998. Strain partioning along the Himalayan arc and the Nanga Parbat antiform. *Geology,* **26**, 791-794.

Shanker, D. Kapur, N., Singh, B. 2002. Thrust-wedge mechanics and coeval development of normal and reverse faults in the Himalayas. *Journal of Geological Society of London,* **159**, 273-280.

Tapponier, P., Mercier, J.L., Armijo, R., Tonglin, Han, Ji, Z. 1981. Field evidence for active normal faulting in Tibet. *Nature,* **294**, 410-414.

Upreti, B.N., Le Fort, P. 1999. Lesser Himalayan crystalline nappes of Nepal: problem of their origin. *In:* Macfarlane, A., Quade, J. & Sorkhabi, R. (eds.), *Geological Society of America, Special Paper,* **328**, 225-238.

Yin, A. 2000. Mode of Cenozoic east-west extension in Tibet suggesting a common origin of rifts in Asia during the Indo-Asian collision. *Journal of Geophysical Research,* **105**, 21745-21759.

Yoshida, M., Igarashi, Y., Arita, K., Hayashi, D., Sharma, T. 1984. Magnetostratigraphy and pollen analytic studies of the Takmar series, Nepal Himalayas. *Journal of Nepal Geological Society,* **4**, 101-120.

APPENDIX

The critical cohesive strength (Mandl & Shippam 1981) can be used to locate the area where the rock is likely to fail under shear. This can be observed by adopting Coulomb type failure criterion as shown by Jaeger & Cook (1979). For shear failure criterion,

$$|\tau| = c + \mu\sigma \quad (1)$$

$$|\tau| - \mu\sigma = c \quad (2)$$

where σ, τ and c are normal stress, shear stress and cohesive strength respectively while μ is the coefficient of internal friction angle. The normal and shear stress across the plane whose normal is inclined at β to σ_1 are

$$\sigma = \frac{(\sigma_1 + \sigma_3)}{2} + \frac{(\sigma_1 - \sigma_3)}{2}\cos 2\beta \quad (3)$$

$$\tau = -\frac{(\sigma_1^2 - \sigma_3)}{2} sin2\beta \quad (4)$$

where σ_1 and σ_3 represent maximum and minimum compressive stresses respectively.

Using equations (3) and (4) in (2) we obtain value of $|\tau| - \mu\sigma$ as

$$\frac{(\sigma_1 - \sigma_3)}{2}(sin2\beta - \mu\cos 2\beta) - \frac{\mu(\sigma_1 + \sigma_3)}{2} \quad (5)$$

The maximum value of this equation is a function of β and is obtained when

$$tan2\beta = -\frac{1}{\mu}$$

So that 2β lies between 90° and 180° and

$$sin2\beta = (\mu^2 + 1)^{-\frac{1}{2}}, \cos 2\beta = -\mu(\mu^2 + 1)^{-\frac{1}{2}} \quad (6)$$

From equations (5) and (6) the maximum value of $|\tau| - \mu\sigma$ is

$$\frac{(\sigma_1 - \sigma_3)}{2}(\mu^2 + 1)^{\frac{1}{2}} - \frac{\mu(\sigma_1 - \sigma_3)}{2}$$

Failure will occur when this is equal to c,

$$\sigma_1\left[(\mu^2 + 1)^{\frac{1}{2}} - \mu\right] - \sigma_3\left[(\mu^2 + 1)^{\frac{1}{2}} + \mu\right] = 2c \quad (7)$$

Since $\mu = tan\phi$, equation (7) can be written as

$$\sigma_1(1 - sin\phi) - \sigma_3(1 + sin\phi) = 2c\cos\phi$$

where ϕ and c are the friction angle and cohesive strength respectively. By this equation we can calculate the cohesive strength using friction angle for each layer and consequently we can locate the potential failure area in the model.